Journal of Cleaner Production 315 (2021) 128194

Contents lists available at ScienceDirect

Journal of Cleaner Production

journal homepage: www.elsevier.com/locate/jclepro

Air quality mapping and visualisation: An affordable solution based on a vehicle-mounted sensor network

Pedro Santana[a,b,*], Alexandre Almeida[a,c], Pedro Mariano[d], Carolina Correia[d], Vânia Martins[d], Susana Marta Almeida[d]

[a] Instituto Universitário de Lisboa (ISCTE-IUL), Portugal
[b] Information Sciences and Technologies and Architecture Research Center (ISTAR-IUL), Lisboa, Portugal
[c] Instituto de Telecomunicações, Lisboa, Portugal
[d] Centro de Ciências e Tecnologias Nucleares (C2TN), Instituto Superior Técnico, Lisboa, Portugal

ARTICLE INFO

Handling editor: Cecilia Maria Villas Bôas de Almeida

Keywords:
Air pollution
Air quality
Human exposure
Mobile sensor networks
Scientific data visualisation
Awareness

ABSTRACT

This paper describes a prototype of the ExpoLIS system, which aims at: (1) informing citizens regarding the air quality of their surroundings and how to cope with it (e.g., choosing commuting routes according to a health model); and (2) gathering dense spatiotemporal air quality data to support the empirical work of environmental experts. The system is composed of: (1) an affordable and custom vehicle-mounted sensor network for air quality monitoring; (2) a server to store, process, and map all gathered geo-referenced sensory data; and (3) a set of user-centred visualisation and prediction services tailored for citizens and environmental experts. Experimental validation of each component of the proposed system shows that the current prototype is capable of tracking spatiotemporal air quality changes and of providing users with access to these events via a set of interfaces. The results show evidence of a strong correlation in static situations (R^2 of 0.96 for PM2.5) between the proposed low-cost all-weather system and a high-cost equipment with no weather protection. The results also show a weaker correlation (R^2 of 0.57 for PM2.5), but still satisfactory, in dynamic settings. In short, this paper presents experimental evidence that supports the claim that the ExpoLIS system is feasible and valuable to both citizens and environmental scientists.

1. Introduction

Urban air pollution is known to be one of the most significant environmental stress factors, as poor air quality levels are strongly associated with increased morbidity and mortality (Almeida et al., 2014; Pope et al., 2011). Despite the increasing awareness among citizens and decision makers about the importance of maintaining high standards of air quality, the current levels of exposure to air pollution are still above the limits defined by the European Legislation and the World Health Organization (EEA, 2019). Therefore, it is of utmost importance to develop all possible strategies in order to mitigate this health problem. To devise such strategies, scientific knowledge regarding pollution phenomena needs to be strengthened or reinforced from empirical evidence, that is, air quality field observations. Once acquired, these data can be provided to citizens with the goal of raising their awareness to the air pollution problem and, for those that are already aware, to help them planning their daily lives in a way that exposure to pollution is reduced as much as possible.

Air quality field observations are typically focused on monitoring airborne pollutants, as these have significant impacts on human health. To this purpose, fixed monitoring stations are often employed. However, although highly accurate, these monitoring stations cannot be installed in large numbers, mostly because of their high acquisition and maintenance costs. As a result, the air quality data points generated by fixed monitoring stations exhibit low spatial density (Carullo et al., 2007). In addition, these stations are equipped with certified devices that are expensive, rather large, and require qualified personnel to ensure the quality of their measurements. The outcome is that, without being able to densely monitor air pollution across the whole inhabited environment, instead of only around a set of key locations, citizens and environmental experts are unable to accurately correlate human activity and environment topology with the spatiotemporal distribution of air pollution. This inaccurate determination of personal exposure to air pollution can bias health risk assessments, affecting the validity of

* Corresponding author. Instituto Universitário de Lisboa (ISCTE-IUL), Portugal.
E-mail address: pedro.santana@iscte-iul.pt (P. Santana).

https://doi.org/10.1016/j.jclepro.2021.128194
Received 14 February 2021; Received in revised form 25 June 2021; Accepted 30 June 2021
Available online 3 July 2021

epidemiological and toxicological studies (Peng and Bell, 2010). Revolutionary advances in sensor technologies for air pollution monitoring provide the potential to cope with this limitation. For example, wireless networks of low-cost sensing nodes offer a solution to increase the coverage area and the temporal resolution of the monitoring process, which can be amplified if the sensing nodes are mounted on mobile platforms (Chatzidiakou et al., 2019) (please refer to (Yi et al., 2015) for a survey on wireless sensor networks for air pollution monitoring). In accordance with Shindler (2021), these mobile sensor networks can complement the data generated by accurate fixed stations, making it possible to know the pollution level anywhere and in real-time. Nevertheless, sensor data validation is required if high data quality is to be ensured (Ripoll et al., 2019). Moreover, Linh et al. (2020) highlight the use of low-cost sensors to assist in the creation of emission inventories of pollutants and detection of pollution hotspots without significant capital investments.

As part of the ExpoLIS project, the main contribution of the present study is the development of an affordable and custom vehicle-mounted sensor network for air quality monitoring, enabling the gathering of sensory data with both spatial and temporal significance. Inspired by the early work of Hasenfratz et al. (2015), to ensure coverage and reliability of the monitoring process, the core of the network is to be deployed on vehicles used for public transportation. However, instead of relying on streetcars, as assumed by Hasenfratz et al. (2015), our system has been designed towards city buses, which offer a more flexible and wider range of operation. To handle the fact that the rooftop of city buses are often bare naked, in opposition to streetcars, our system needs to be able to sample air under harsh weather conditions. Interestingly, this challenge pushed us to create a novel design for air sampling, which we believe can benefit other related projects.

Although the idea of exploiting city buses to transport air pollution monitoring devices has already been addressed by Devarakonda et al. (2013) and Gao et al. (2016), these early solutions were not prepared to handle all-weather operation. In addition, our system also includes a server-side, whose task is to control the sensor network, gather the produced sensory data, process and map it, and provide a set of novel graphical services for its remote exploitation by users (citizens and environmental experts). These graphical services intend to foster the citizens' awareness about air pollution and to help them planning daily commutes so as to reduce exposure to air pollutants, and, consequently, improve health and well-being. The routing service chooses paths that trade-off human exposure to pollution, path length, and travel time. Moreover, the system also aims at providing relevant up-to-date information for decision makers, with the goal of supporting urban planning policies. It is known that commuting accounts for a short amount of daily time, nevertheless, the contribution to the daily personal exposure to pollutants may be disproportionally high (Faria et al., 2020), depending on local pollution and traveling mode (Correia et al., 2020). Therefore, exposure assessment during commuting remains a major public health issue in urban areas, deserving increased attention. The present study contributes to this global effort.

In summary, the ExpoLIS system contributes with a novel and affordable vehicle-mounted sensor network, together with a set of related graphical services designed for citizens who wish to plan daily trips, minimising exposure to air pollution. This article extends the conference paper (Santana et al., 2020) and is organised as follows. In Section 2, the ExpoLIS system is described. Section 3 presents the results obtained with the proposed system in a set of field experiments. Finally, Section 4 draws some conclusions and presents future work directions.

2. Proposed system

2.1. System architecture

ExpoLIS is a layered, distributed, and heterogeneous system, whose purpose is to collect, map, and predict geo-referenced air quality data in urban environments, as well as to provide citizens with intuitive access to these data when planning daily commutes, fostering an healthier lifestyle. To meet these goals, ExpoLIS is divided in three layers, as depicted in Fig. 1.

The ExpoLIS system's bottom layer includes all mobile sensor nodes, which are distributed across multiple personal and public vehicles. These sensor nodes sample the environment autonomously, and communicate the gathered data to the ExpoLIS server via a wireless channel over the internet.

The ExpoLIS server, located in the middle layer of the architecture, is responsible for collecting all sensor data, storing it in a geographical database, and to provide citizens with web-based access to these data. The server is also responsible for the coordination of the sensor nodes so as to ensure system-wise robustness. The top layer of the system includes all ExpoLIS users, which, through a set of mobile graphical tools, access individual and spatiotemporal aggregated air quality data stored in the server's database. These tools also allow the user to plan routes within the monitored region by weighing traveling distance and air pollution exposure. Spatiotemporal air quality predictions, given historical data, can also be accessed by the user (described elsewhere (Mariano et al., 2020)). The connectivity between user graphical tools and the ExpoLIS server happens over the internet and, thus, can be either wired or wireless.

2.2. Sensor node

This section presents the mechanical (air sampling device and enclosing case), hardware (electronics and air quality sensing devices), and control software components (sensor data acquisition, storage, and transmission) of ExpoLIS sensor nodes.

2.2.1. Design requirements

The sensor node's design must ensure that the air quality sensors are in contact with an adequate air flow, while dealing with the following constraints: (1) electronic components need to be protected against harsh weather conditions; (2) the sensor node needs to be as small as possible to render it inconspicuous and promote future deployment in small vehicles (e.g., bicycles); and (3), to enable massive deployment, the sensor node needs to be affordable, to rely mostly on consumable equipment, and to be based as much as possible on open-source and open-hardware components.

2.2.2. Mechanics: design

Fig. 2 presents two views of a three-dimensional conceptual model of the sensor node. This design reflects the need for achieving the smallest occupied bounding volume capable of housing all air quality sensors, air sampling mechanism, and support electronics. The bounding box of the sensor node has a width, a height, and a depth of 38 cm, 22 cm, and 9 cm, respectively. The sensor node's design reflects the assumption that the device needs to be fixed on the roof of a vehicle as distant from the vehicle's exhaust pipes as necessary so as to ensure that these cause no direct influence on the air quality observations.

The air sampling device is based on a simple hollow tube with a diameter of 5 cm, which is set parallel to the vehicle's motion direction, with the air inlet facing forward. This configuration allows the surrounding air to easily enter the tube and flow through it. As the air flows through the tube, it gets in touch with the air quality sensors, which are inserted in four holes on the top of the tube, along its longitudinal axis. With this placement, the sensors face downwards, which results in a passive protection, by gravity, against water droplets, moister, and dirt.

Further protection against rain has been brought in by designing the tube's air inlet with a downwards U-like shape. To ensure that any condensed water or water droplets that get into the tube do not accumulate therein, the tube is slightly tilted. The drained water, as well as, the airflow, are exhausted via an air outlet, implemented with a downwards curved elbow-like hollow tube. This shape aims at

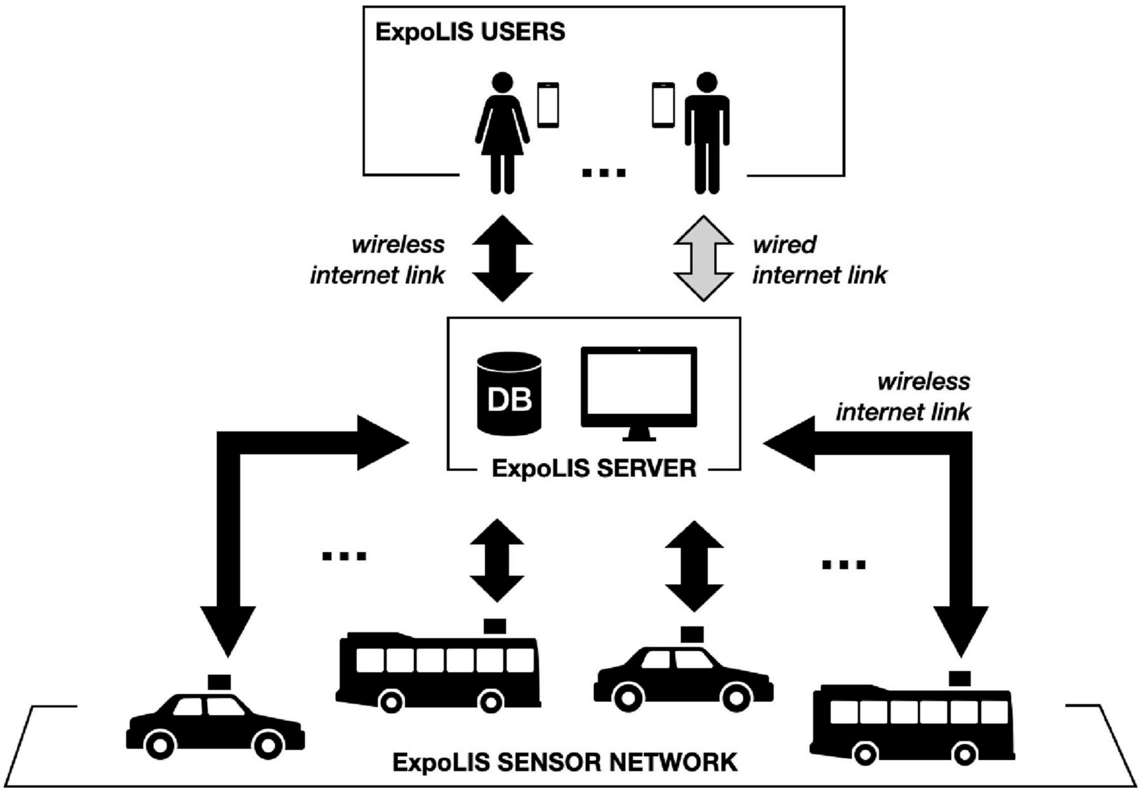

Fig. 1. ExpoLIS layered approach. Black and grey arrows correspond to wireless and wired internet links, respectively. Sensor nodes are represented as black-filled small rectangles placed on each vehicle's roof.

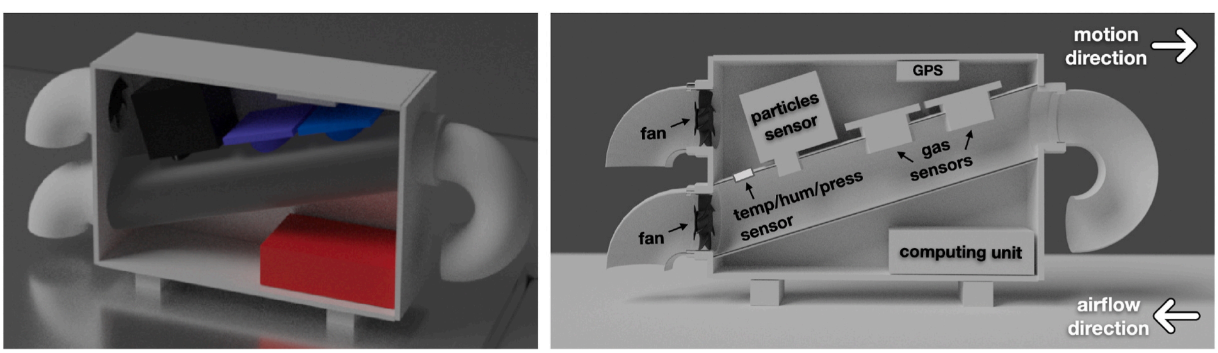

Fig. 2. Three-dimensional conceptual model of the sensor node's mechanical design (Left). Cross-section of the three-dimensional model (Right), with vehicle's motion direction and resulting airflow direction represented by two white arrows.

preventing water from entering the hollow tube when the vehicle is being washed.

As the vehicle moves, air flows naturally through the hollow tube, thus being conveniently sampled. However, when the vehicle is stopped, an active airflow inducing mechanism is required. To this purpose, an air extraction fan capable of producing an airflow of 3 CFM has been placed at the air outlet. Solar exposure may heat the air inside the sensor node to the point of damaging the equipment. To avoid this, an active cooling mechanism composed of a second airflow outlet with a dedicated air extraction fan was added. Fig. 3 depicts the airflow within the sensor node.

To geo-reference all data points, a GPS device is placed at the top face of the sensor node's enclosure, ensuring a proper sky view.

2.2.3. Mechanics: analysis

OpenFOAM (Weller et al., 1998), a Computational Fluid Dynamics (CFD) analysis software package, was used to determine the ability of

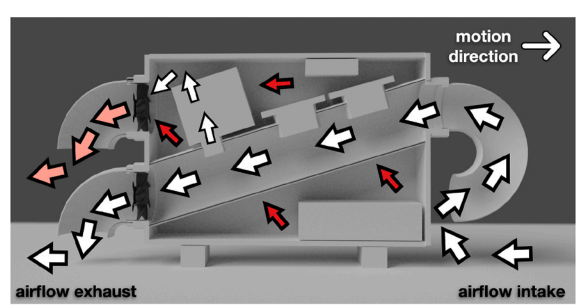

Fig. 3. Airflow within sensor node. White arrows represent the main airflow going through the hollow tube; a portion of this airflow is pumped in the particulate sensor. Red arrows represent heated airflow. Pink arrows represent the exhaust of a mix of heated airflow and airflow that passed through the particulate sensor.

the sensor node to properly sample the surrounding air while in motion. For this purpose, the analysis was executed using the conceptual model depicted in Fig. 2. To check the possibility of the sensor node to sample the air in a mechanically passive way, the air extraction fans were removed from the conceptual model used in the CFD analysis.

The simulations were run assuming that the vehicle moves at 10 m/s (36 km/h). This was implemented in the CFD analysis software package by putting the vehicle at zero speed and forcing a constant 10 m/s airflow incoming from a vertical wall-like inlet perpendicular to the motion direction.

Representative results from the CFD analysis can be depicted in Fig. 4. These results show that the sensor node's shape combined with the incoming airflow direction generate a considerable pressure difference between the sensor node's frontal face (the one holding the air inlet) and the sensor node's rear face (the one holding the air outlet). This pressure difference induces an air flow that enters the sensor node through the air inlet, crosses the hollow tube, and leaves the sensor node via the air outlet. Hence, when the vehicle is in motion, the device is able to enforce an airflow through the air quality sensors, even in the absence of air extraction fans. The airflow's vertical and horizontal speed components depicted in the figure support this conclusion.

The CFD analysis also revealed that the air's horizontal speed across the hollow tube is approximately 2 m/s, although the vehicle is moving at 10 m/s. In other words, the sensor node operates as an airflow damper. Interestingly, this damping effect contributes positively to the robustness of the analyses performed by the air quality sensing devices when facing varying vehicle speeds. In particular, the particulates sensing device uses an embedded fan to pull air into an internal chamber, in which it performs a laser-based analysis. If the air speed in the hollow tube is too high, the inertia of heavier particles can hamper the device from pulling them in. Similarly, if the air flows on the gas sensors' surfaces too rapidly, these may be unable to properly analyse the air volume.

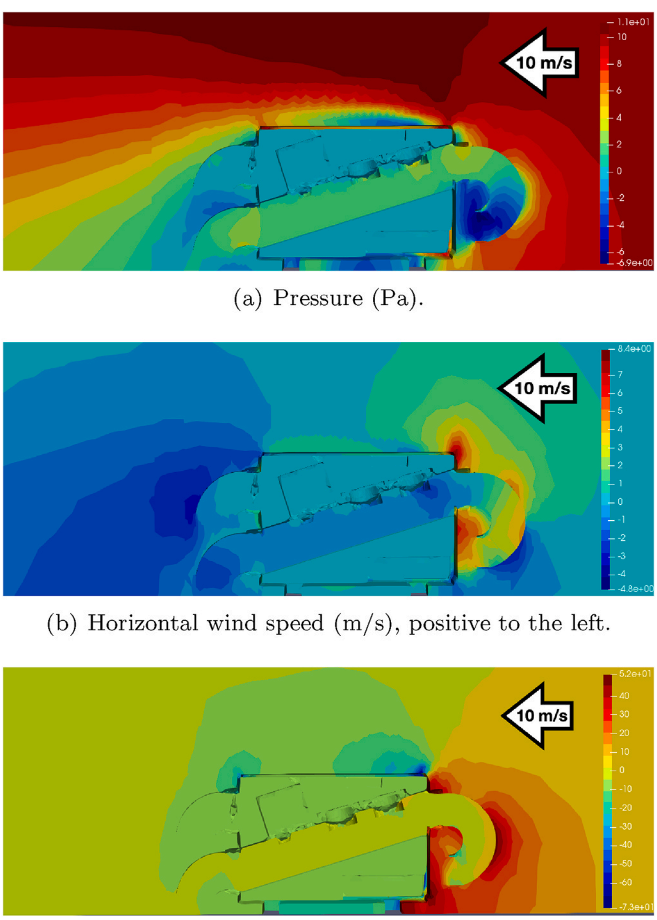

(a) Pressure (Pa).

(b) Horizontal wind speed (m/s), positive to the left.

(c) Vertical wind speed (m/s), positive upwards.

Fig. 4. Sensor node's CFD analysis without air extraction fans. Incoming wind's direction represented by white arrows.

2.2.4. Hardware: architecture

The sensor node's hardware is depicted in the block diagram of Fig. 5 and all the sensors, model, manufacturers, and prices are listed in Table 1. As shown in the table, building an ExpoLIS sensor node roughly amounts to 630 USD. This value, although already reasonably low, is expected to be reduced even further as a result of the growing demand and competitiveness in the low-cost air quality sensors market. In fact, this market is very active, with several manufacturers launching new products at an interesting pace.

The sensor node's core unit consists of a RaspberryPi 3B+ (RPi3) single board computer, with a 1.4 GHz 64-bit quad-core processor, a dual-band wireless LAN, including WiFi and Bluetooth 4.2/BLE. Even though the newer RaspberryPi model 4 is available, we found the previous model to be a better choice due to its reduced energy consumption while providing the necessary resources and computing power to process all sensory data and maintain robust wireless communications. An alternative would be to select a RPi Zero; however, the RPi3 has onboard support for Bluetooth LE (BLE) and WiFi, whereas the RPi Zero does not. BLE can provide remote configuration access and WiFi (together with an Ethernet port for wired connections), which are essential components for the portability of the solution. Computationally, the RPi3 has double the RAM and three more cores, which is a configuration that expands the possibility of better data processing at the end node. The higher energy consumption of the RPi3, compared with the RPi Zero, is dealt with by making the processor sleep during inactivity periods (passive waiting). The RaspberryPi runs a Linux OS, which is useful in setting up database and MQTT (Banks et al., 2019) local servers.

As vehicles travel through the city, the sensor node tracks its geographic position with a GPS module. In addition, a real-time clock tags all sensor readings with a timestamp. Both of these modules share the I2C protocol. To force an air flow, even when the vehicle is at rest, we use two fans that are controlled by General Purpose Input/Output (GPIO) pins of the RaspberryPi.

The following sections detail the sensing and power supply hardware sub-systems.

2.2.5. Hardware: air quality sensing devices

Each sensor node is equipped with three air quality sensing devices. Two gas sensors from Alphasense provide readings of carbon monoxide (CO) and nitrogen dioxide (NO_2). These fuel cell technology sensors use four electrode compensation and, therefore, can reliably detect very low parts per billion levels (gas concentrations for NO_2 are typically 20 ppb–200 ppb at the roadside). Given that the output of these sensors is an analog voltage, an analog-to-digital converter (ADC) is used to provide the corresponding digital values to the processor. This ADC communicates via an I2C bus. Other sensors to measure barometric pressure, temperature, and humidity share the same bus.

In urban air monitoring, one of the most critical variables is the mass concentration of suspended Particulate Matter (PM). A laser-based optical particle counter OPC-N3 from Alphasense is used to measure particulate matter with aerodynamic diameter equal to or less than 1 μm, 2.5 μm, and 10 μm (PM1, PM2.5, and PM10, respectively). This device communicates with the processing unit via a serial interface (SPI).

2.2.6. Hardware: power supply

Given that each node is installed on a vehicle (e.g., a city bus), we can take advantage of the vehicle's 12 V battery supply. However, this supply can fluctuate between 12 V and 24 V and, for this reason, we chose an isolated DC-DC converter with a wide input range. Its 5 V/3 A output powers all node's electronic components. At boot time, the sensor

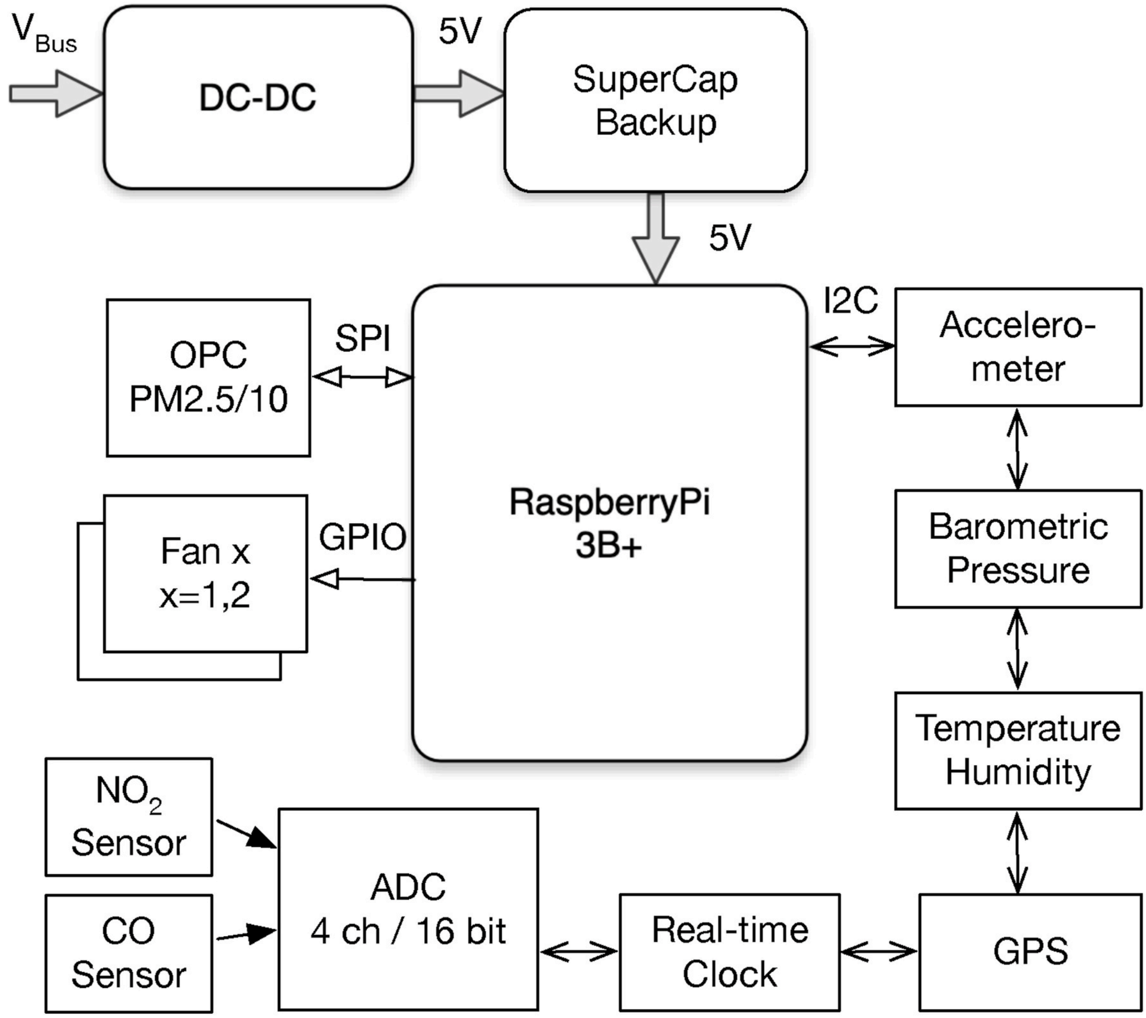

Fig. 5. Block diagram for the sensor node's hardware.

Table 1
Description of the sensor node's hardware modules.

Module	Model	Notes	Price (USD)
Computing	RaspberryPi 3B+	Single Board Computer	40
DC-DC	NSD15-12S5	15 W/5 V, 3 A	13
T/H	Adafruit SHTC3	(I2C: 0 × 70)	5
ADC	Adafruit ADS1115	4 ch/16 bit (I2C: 0 × 48)	12
CO	Alphasense CO–B4	336 mv/ppm	60
NO_2	Alphasense B43F	165 mv/ppm	60
Particulate	Alphasense OPC-N3	PM (SPI)	395
GPS	Adafruit PA1010D	(I2C: 0 × 10)	25
RT Clock	Adafruit DS1307	(I2C: 0 × 68)	7
Pressure	Adafruit LPS25	(I2C: 0 × 50)	5
Fan	EF30080S2-E00U	30 × 8 mm 3 CFM	7
D1	MBRA210L	Schottky diode	0.5
D2, D3	LM6610	Ideal diode	0.5
Boost	TPS61023	Boost converter	0.8

node consumes 1 A, after which it stabilises around 350 mA, which opens up the possibility of the sensor node to be powered by photovoltaic cells.

2.2.7. Control software: architecture

The key components of the sensor node's control software running on the RaspberryPi and respective connectivity can be depicted in Fig. 6. The core inter-component communication medium is based on MQTT, which is a lightweight publish-subscribe messaging protocol designed for robust operation over unreliable communication networks. Every *Sensor Node i*, equipping a given vehicle *i*, executes a persistent Python script, *Sensor Node i Manager* (more details in Section 2.2.8), which is responsible for sensor data acquisition, pre-processing, local storage, and transmission to the ExpoLIS server.

Communications between sensor nodes and the ExpoLIS Server are established over 3G/4G or WiFi internet links, depending on each one's availability. Data transmission to ExpoLIS Server is carried out via MQTT messages, whose payload is the data to be transmitted. These messages are published on a set of ExpoLIS-custom topics (more details in Section 2.2.8) available at the MQTT Broker running on the ExpoLIS Server, recurring to the Paho MQTT Python client library. Messages are redirected to a publicly available MQTT Broker in case the ExpoLIS-dedicated version fails to respond. ExpoLIS-related MQTT messages are set to maximum MQTT quality of service available, i.e., two. This option reduces the probability of losing relevant exchanged data in unreliable networks.

A set of processes running at the ExpoLIS server are responsible for subscribing the MQTT topics, through which the processes collect all data produced by the sensor network. Based on the gathered data, these processes provide a set of services (e.g., air quality maps, health-optimal routes) to remote users via Graphical User Interfaces (GUI) (see Section 2.4).

To configure and coordinate the activities of each sensor node, the ExpoLIS Server publishes specific MQTT messages to ExpoLIS-custom topics on the MQTT Broker running on the server. Each sensor node

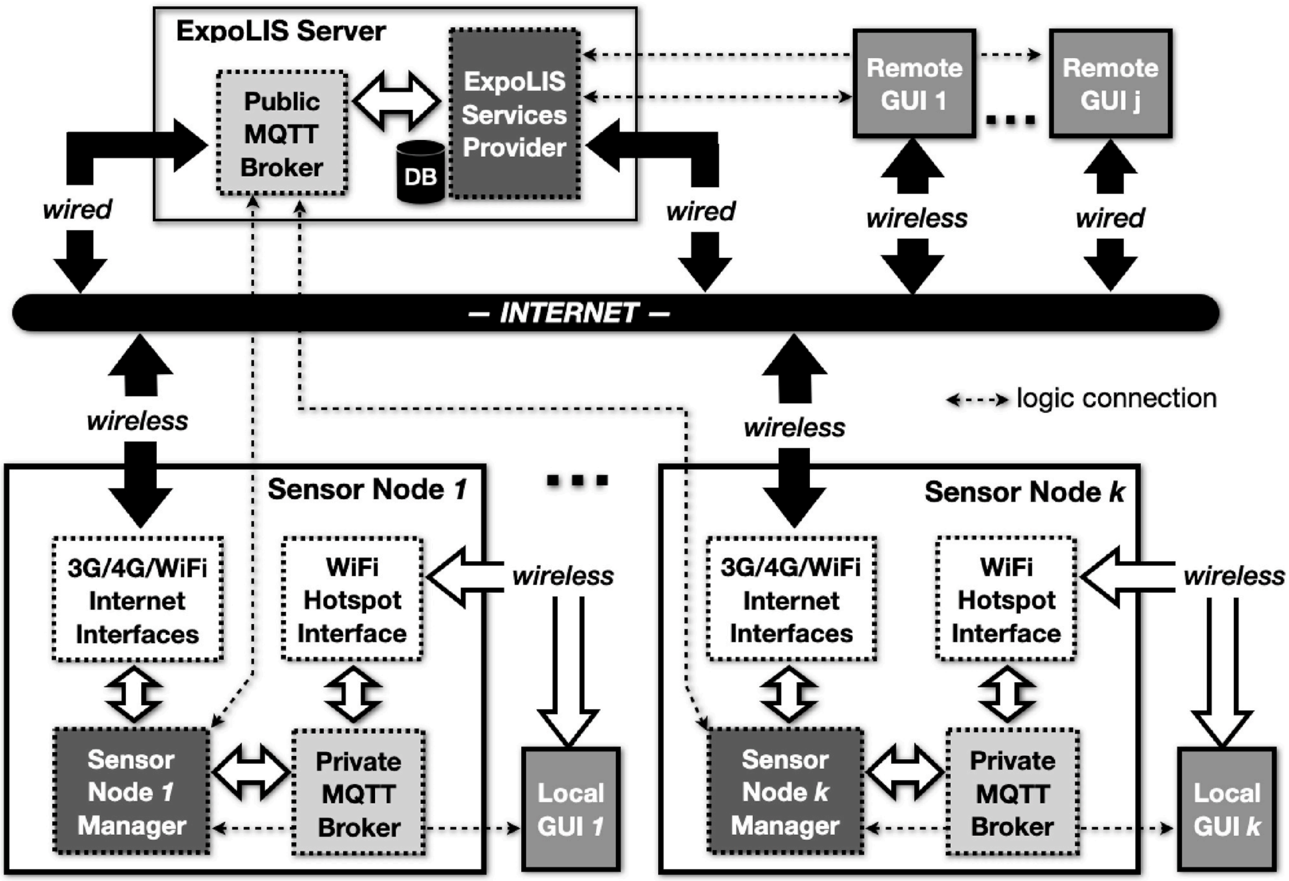

Fig. 6. Sensor node's software architecture. Different solid boxes represent different software components being executed on separate machines. Dashed boxes within a given solid represent software sub-components running in the same machine. Filled and unfilled large arrows correspond to internet and intranet links, respectively. Thin dashed arrows represent logic connections between two components, i.e., application-level interactions.

receives its associated messages by subscribing the respective MQTT topic. This blackboard-like approach, in alternative to sending messages directly to their intended recipient(s), circumvents the need for keeping every sensor node's public address, thus increasing the system's resilience to network configuration changes.

It is not always possible for a sensor node to access the MQTT Broker running at the ExpoLIS Server. For instance, a sensor node deployed as a fixed monitoring station in an underground parking lot may not be able to access the internet via WiFi/3G/4G. To handle these situations, every MQTT message that is sent to the public MQTT Broker hosted by the ExpoLIS Server is simultaneously sent to a local/private MQTT Broker running at the sensor node itself. To enable access to these locally published MQTT messages, the sensor node is also configured as a WiFi hot-spot, thus delivering its own local wireless network. A nearby machine that connects to this wireless network gains access to the local/private MQTT Broker and, consequently, is capable of subscribing to the topics published therein.

2.2.8. *Control software: Sensor Node Manager*

The main process running in the sensor node's computing unit is a python script called Sensor Node Manager (SNM). The SNM is multi-threaded and persistent, in the sense that it endlessly runs while the sensor node has power. As mentioned, sensor nodes communicate with MQTT local and public brokers (depending on the network configuration) in order to cast sensor readings, cast sensor node status, and receive supervision and control commands, all as MQTT messages. Fig. 7 presents the bundle of MQTT topics that are associated to each *Sensor Node i*. The goal of using topic bundles associated to each sensor node is to reduce the overhead imposed by publishing and subscribing MQTT messages.

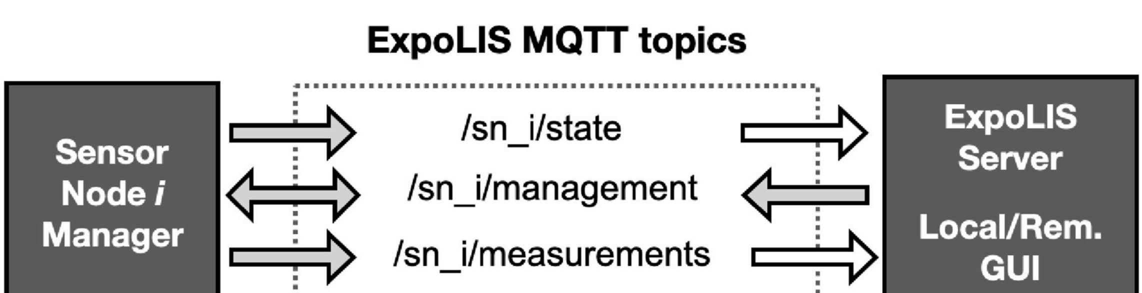

Fig. 7. Bundle of MQTT topics related to each *Sensor Node i*. Unidirectional grey and white arrows represent publish and subscribe requests, respectively. Bidirectional arrows represent coexisting publish and subscribe requests.

The SNM recurs to a set of open-source and custom device drivers to periodically (by default 1 s) gather sensor data. These data are immediately geo-referenced with GPS data and time-tagged according to a local real-time clock. At the same pace, the SNM filters the gathered sensor data for smoothing and removal of outliers. The SNM packs the gathered geo-referenced and time-tagged raw and filtered sensor data and adds these as payload of MQTT messages, which are published in the measurements topic of the local or public MQTT Broker, depending on the network configuration. The payload of these messages is extended to include a message unique identifier (an integer number incremented at each new message) and key configuration parameters (e.g., sensor data filtering parameters) to provide context in further data analysis.

The SNM also publishes operational state information to the state topic. These messages include asynchronous acknowledgement of incoming commands via MQTT messages as well as the sensor node's current state (e.g., whether it is logging sensor data to local text log files). The payload of the MQTT messages published in measurements topic is locally stored in volatile circular buffers (for later use by the SNM), as well as in persistent text log files, when requested via a MQTT message for later download.

The SNM subscribes a management topic in order to receive control commands (e.g., restart/reboot the process/machine, start/stop sensing and logging) and configuration commands (e.g., sensor data filtering setup, WiFi access setup, real time clock setup), which are either automatically generated by the ExpoLIS Server or triggered by the user through the ExpoLIS Configuration and Supervision Tool (see Section 2.4).

Gas sensing devices exhibit a slow integrative dynamics, which renders them naturally robust to the presence of outliers and high-frequency noise. However, that is not the case with particulate sensing devices, including the one selected in the ExpoLIS project. Thus, it is essential to smooth the data generated by particulate sensors and to detect and remove existing outliers. For this purpose, the SNM filters all three particulate sensor outputs, i.e., PM1, PM2.5, and PM10, with independent Kalman Filters, under the simplifying assumption that the three are uncorrelated.

In each sampling iteration k, each Kalman Filter updates an estimate of the true mass concentration of a given particulate type (i.e., PM1, PM2.5, or PM10) based on its previous estimate, a system's dynamical model, and the current mass concentration observation made by the sensor. The higher the uncertainty of the sensor observation is expected to be, represented as a covariance matrix, the less it is taken into account in the estimate update.

Typically, in each time-step k, Kalman Filters assume that an observation o_k is polluted with zero mean Gaussian white noise, r_k, with covariance $R_k : r_k \sim \mathcal{N}(0, R_k)$. However, the considerable magnitude and frequency of outliers present in the sensor data obtained with the selected particulate sensing devices are insufficiently filtered out under such assumption. To circumvent this limitation, the Kalman Filters in the SNM assume an alternative formulation of the observation covariance. Concretely, whenever in the likely presence of an outlier (resulting from either endogenous or exogenous events to the sensor), an heuristically-defined expected covariance contribution γ is added to the sensor's background covariance, α:

$$R_k = \alpha + \gamma \log\left(\frac{\max(o_k, o_{k-1})}{\min(o_k, o_{k-1})}\right) \quad (1)$$

The heuristically-defined covariance contribution is modulated according to the ratio of change between the previous and the most recent observations. The goal is to ensure that, the stronger the change in the observation, the higher its associated covariance. To warrant that strong outlier events do not saturate the filter, this contribution is squeezed by the log function.

Currently, α and γ are empirically tuned so as to find a proper smoothing strength. Desirably, these parameters should be automatically updated, in run-time, by sampling the sensor's natural statistics. Fig. 8 plots raw and corresponding Kalman filtered particulate sensor data during a test, run with Prototype V_1 (see Section 2.2.10) mounted on a moving car's roof. The plot shows that the implemented Kalman Filter manages to smooth the sensor data, to reject outliers, and, still, to robustly track the signal. Outliers are clearly visible in the plots as extreme short-term peaks.

2.2.9. *Control software: error recovery*

Deployed sensor networks are intended to operate autonomously throughout long periods of time. This demands for resilient sensor nodes, capable of detecting and recovering from operation errors. To this aim, the SNM's main thread is responsible for periodically (every 10 s) reporting that it is alive by touching a local empty file. A minute-wise activated watchdog *cron* job monitors the modification time of this file and forces a restart of the SNM process at the operating system level whenever the file gets older than a minute. However, if the file gets older than 5 min, then the watchdog *cron* job forces a reboot of the computational unit.

Although the MQTT quality of service is set to the highest level (two), experience shows that when the network fails for over 1 min, the loss of messages is very likely to occur. To cope with these cases, a script running at the ExpoLIS Server subscribes the measurements topic associated to the sensor node and searches for gaps in the unique identifiers of the received messages, which are sequential in the absence of gaps. Then, all missing identifiers are packed and published as a MQTT message in the management topic of the corresponding sensor node. Whenever one of these messages is received by the SNM, the later reacts by re-publishing the missing messages in the measurements topic. To be able to re-publish these messages, the SNM locally stores published messages in a volatile circular buffer with 1 h capacity.

2.2.10. *Prototypes*

Given the positive results obtained with the CFD analysis, the conceptual model of the sensor node has been implemented as a functional prototype (including electronics and software), which can be depicted in Fig. 9(a). This prototype, hereafter Prototype V_1, is based on a standard IP65 electronics plastic box. The hollow tube is based on a standard PVC tube, whereas the curved tubes are consumable plastic toilet plumbing pipes. All these components are consumer-based to ensure affordability and fast prototyping. All elements junctions are bonded and protected with silicone and aluminium tape for additional mechanical strength and waterproofing.

With Prototype V_1, the water-resilience assumptions of the air sampling system were tested, with positive results, by projecting water jets in all meaningful directions over periods of several minutes, assuming the vehicle's roof as the preferred mounting location. As it will be shown (see Section 3), this prototype also showed that the hardware and control software components perform adequately. Moreover, it allowed us to compare the accuracy of the sensor node with existing sensing alternatives.

To facilitate large-scale reproduction and to improve mechanical robustness and water-tightness, the design behind Prototype V_1 was refined, resulting in Prototype V_2 (see Fig. 9(b)). In Prototype V_2, both U-like air inlet and the elbow-like air outlet are attached directly to the hollow tube, rather than to the sensor node's walls (see Fig. 10). This reduces the chances of water flooding into the sensor node. Moreover, in this second version, the tube, the air inlet, and the air outlet, are all standard, attachable, and affordable air conditioning PVC tubes, designed to reduce dust accumulation.

2.3. *ExpoLIS server*

The main component of the ExpoLIS server is a geographical PostgreSQL database with the PostGIS extension, in which all sensor data is stored. Fig. 11 shows a diagram of the tables present in the database

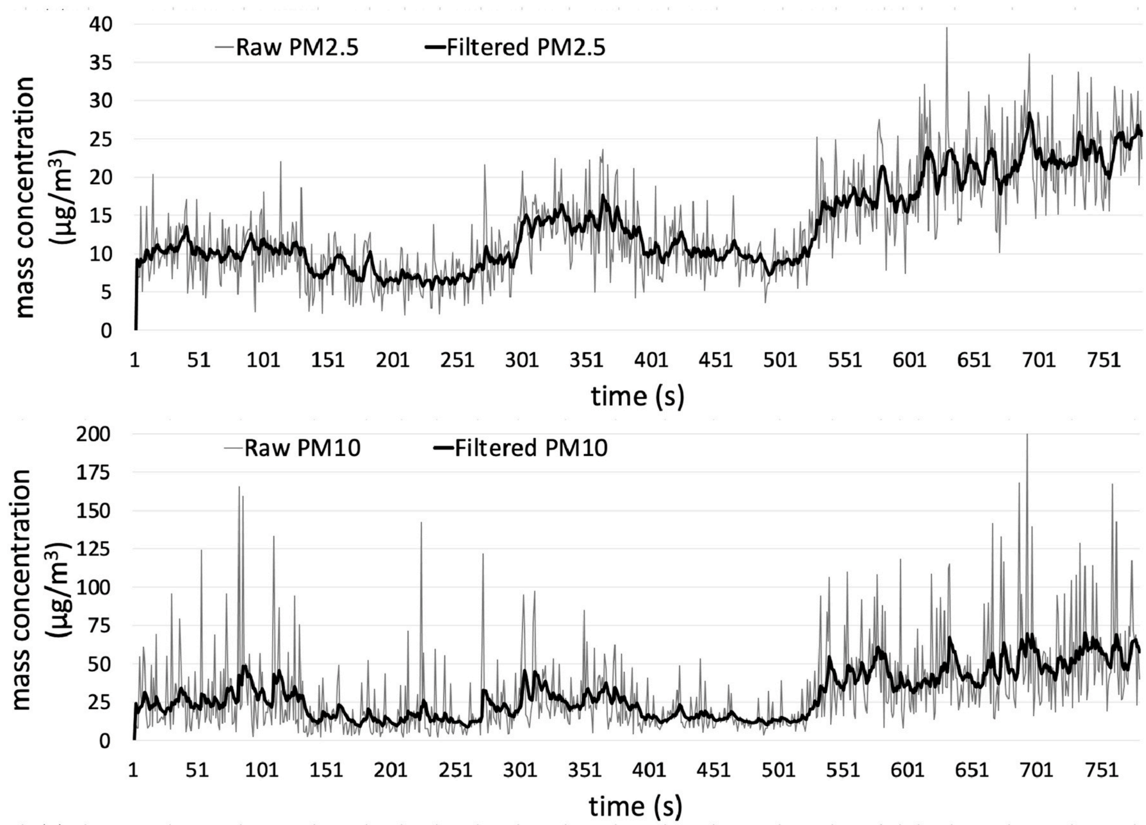

Fig. 8. Raw and Kalman filtered PM2.5 (Top) and PM10 (Bottom) mass concentrations sampled by Prototype V_1 (see Section 2.2.10), mounted on a moving car's roof, while moving in an urban environment (see Section 3), with $\alpha = 20$ and $\gamma = 50$.

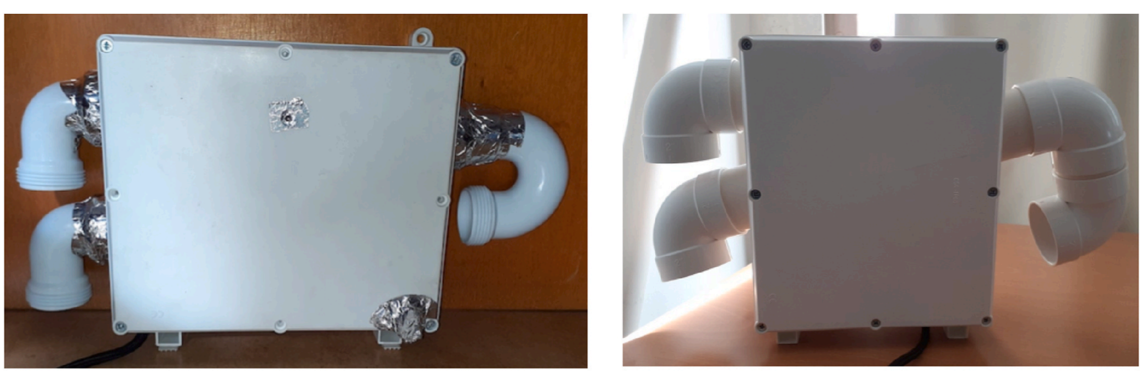

(a) Prototype V_1 (b) Prototype V_2

Fig. 9. Sensor node prototypes.

along with foreign key relations and the fields that are the primary key, labelled with FK and PK, respectively. The database was designed taking into account an heterogeneous network of sensors. As such, each sensor reading is stored in its respective table. In Fig. 11, this set of tables is represented by table measurement_D, where D can be temperature, pressure, PM10, among others.

Besides storing raw sensor data, there are also tables that contain aggregated and interpolated data. The former is represented by table aggregation_S_D_P_R, where S represents the used statistical function (maximum, minimum, average), P represents the time period (hour or day), and R represents the spatial resolution (50 m or 100 m). The latter is represented by table interpolation_M_D_P, where M represents the used interpolation method. The database also contains tables that represent bus lanes, sensor characteristics, and which sensors are deployed on which buses.

To receive sensor data, the ExpoLIS server maintains a MQTT client that subscribes to the measurements MQTT topic as shown in Fig. 7. This client is launched by a script that also performs basic managing tasks on the database, like adding a new sensor node or obtaining a brief report on the stored data.

The ExpoLIS server also includes a routing component that was built upon the Open Source Routing Machine (OSRM) (Luxen and Vetter, 2011). The routing service implemented in this software package uses geographical information stored in Open Street Map format and allows for user defined profiles. These profiles specify which roads can be followed and their weights in the shortest path algorithm, which is a variation of Dijkstra's original algorithm. We have implemented a set of profiles that depend on the sensor data. These profiles were based on the

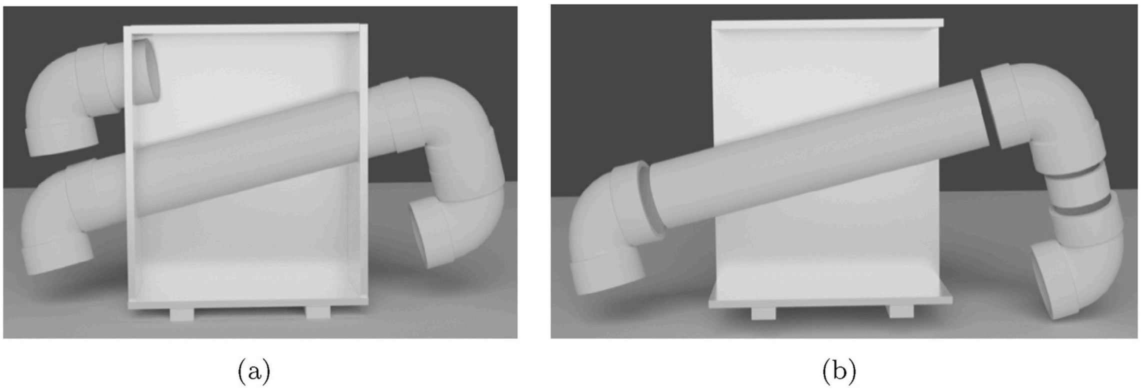

Fig. 10. Air sampling component of Prototype V_2 (a) and its exploded view, with only the hollow tube visible (b).

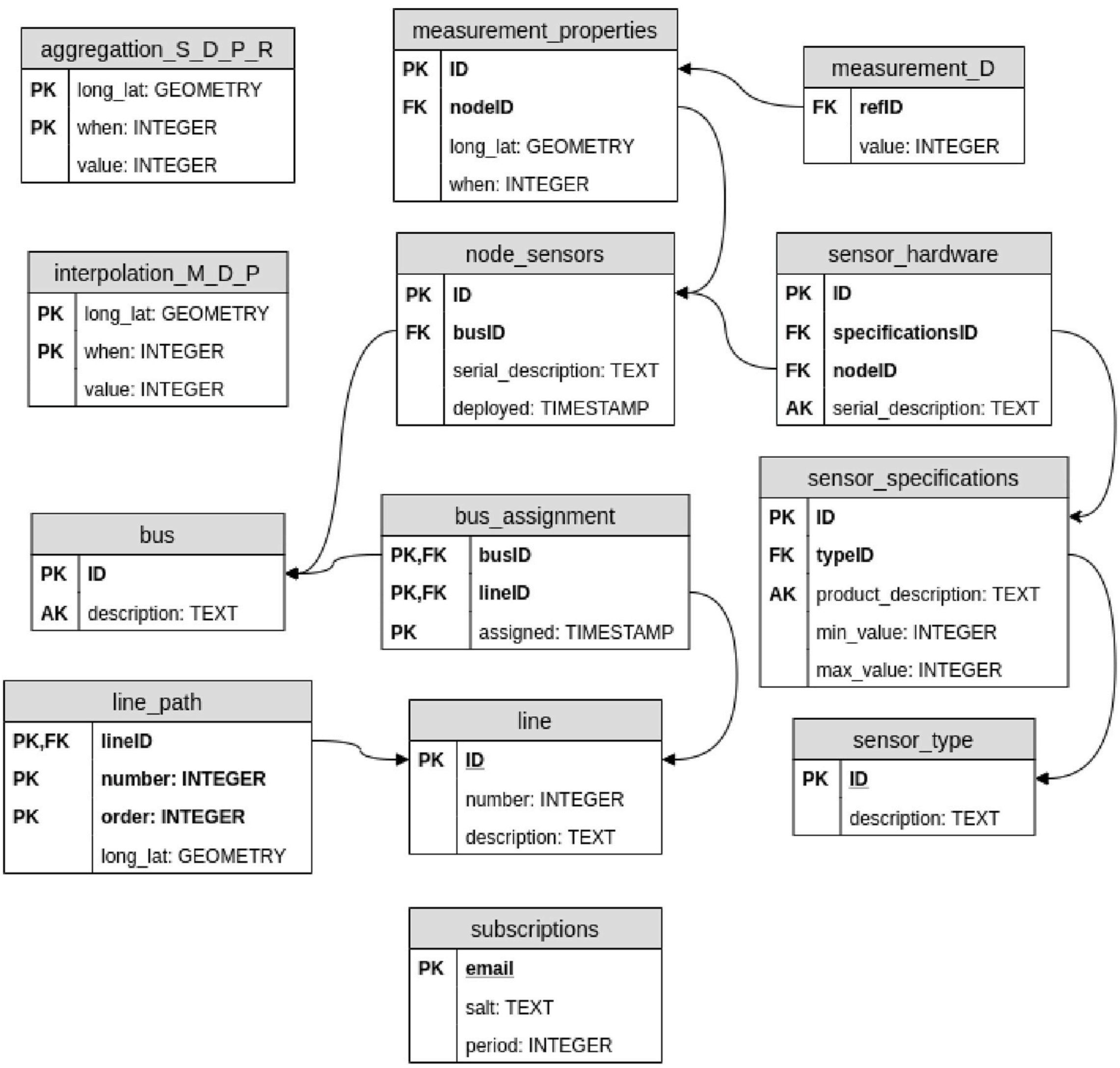

Fig. 11. The entity relation diagram of the tables present in the ExpoLIS database.

ones that are available in the OSRM web site.[1] In particular, there are profiles that take into account paths that can be traversed on foot, by bicycle, or by car. Our profiles modify the road weight according to $w_n = (w_o + \sum_n \max_s v(n, s))/2$, where w_n is the new weight, w_o is the weight that is computed by the OSRM profile, and $\sum_n \max_s v(n, s)$ is the sum (along n points of the road) of the measurements made by sensor s, with the maximum scaled value $v(n, s)$. Our ExpoLIS server thus has 6 routing profiles that depend on the transportation type and on whether pollution is considered or not. Our system differs from previous work on

[1] http://project-osrm.org/.

health-optimal path planning from (Hasenfratz et al., 2015), in which the weight of a road is either its distance or the concentration of ultra fine particles. Instead, our solution allows the user to trade-off both criteria. Moreover, our system benefits from using a versatile community-based open-source solution for path-planning (OSRM), whereas a custom path-planning solution was considered by Hasenfratz et al. (2015).

The ExpoLIS server has a web component that presents a HTML form through which users can download or subscribe to sensor data. Information of which users have subscribed is stored in table subscriptions, as shown in Fig. 11. The web component runs in Apache with the PHP extension.

Another component of the ExpoLIS server is the set of *cron* scripts responsible for computing the aggregated and interpolated data, to update the routing profiles used by OSRM, and to send data to subscribers. These scripts and the source code to create the database were developed in Python.

2.4. *User interfaces*

As mentioned, all data gathered by the sensor network is geo-referenced, time-tagged, and stored in the ExpoLIS server. A set of user interfaces have been implemented to enable user access to these data. To be efficient, these interfaces were designed to fit the specific tasks that users are expected to carry out with them. This involved studying the target audience and involve it as much as possible in the design of the user interfaces and corresponding validation. Concretely, an iterative participatory design approach was followed, in which workshops with environmental experts allowed the development team to refine requirements and interfaces, as well to perform formative tests intertwined with heuristic evaluations.

Four user personas were identified: information-seeker, learner, expert, and developer. An information-seeker primarily represents pollution-aware people who are willing to use air quality information to determine, for instance, which routes should be taken in daily commutes if exposure to air pollution is to be minimised. A learner represents people who are invited to interact with the system using game-like strategies in order to gain air pollution awareness in an engaging way, so that one day the learner becomes an information-seeker. An expert represents researchers and practitioners in the air quality field who need to efficiently gather bulk air pollution data for statistical analysis and model building, given a spatiotemporal window. Finally, a developer represents people from the system's development and maintenance team, who need to monitor, supervise, diagnose, and control each node in the system at run-time.

Fig. 12 illustrates the ExpoLIS graphical user interfaces that were designed with each user persona in mind. The following sections detail these user interfaces.

2.4.1. *Interface for the information-seeker*

To provide access to the collected sensor data by people with pollution concerns, we have developed a mobile application. This tool allows a person to inspect air pollution data using two possible visualisation modes, either in a map or in a chart. Another available feature is the ability to plan routes using the routing component of the ExpoLIS server as described in Section 2.3. By default, the application shows real time data collected by a specific sensor node (Fig. 13 left-most screenshot). An emoticon is used to represent the overall air quality index of the collected sensor data: CO, NO_2, and PM concentrations. A person can select between raw or interpolated data, how it is aggregated, which sensor data to visualise, the time period, if it is constrained to a bus lane or not, the spatial resolution, the geographical location, and the radius of the region to analyse. The left-middle screenshot in Fig. 13 depicts how the map visualisation mode can be configured, whereas the middle screenshot shows the actual map visualisation mode.

The user can specify the mobility means (i.e., on foot, by bicycle, or by car) and whether the exposure to air pollution should or should not be considered as a criterion by the routing system in addition to travel distance, when searching for the best route. Air pollution exposure is computed based on the air pollution data stored in the ExpoLIS server. When the user requests a route that ignores pollution, we use the default profiles provided by OSRM. The right-middle and right-most screenshots in Fig. 13 show an example of the route planner, with *avoid pollution* and *ignore pollution* configurations, respectively.

2.4.2. *Interface for the learner*

In the context of ExpoLIS project, Teles et al. (2020) developed a game-like air quality data visualisation tool based on the Unity game engine (the left-middle representation in Fig. 12 depicts a screenshot of the tool). The game-like nuances of the tool are intended to foster users' engagement in the exploration of air quality sensory data and, ultimately, raise their awareness to air quality and its health impact.

2.4.3. *Interface for the expert*

As mentioned in Section 2.3, the ExpoLIS server contains a web component through which users can search and subscribe to sensor data. Fig. 14 shows the search and subscribe forms. In these forms, an expert can search for sensor data, and receive a link to download the data as a CSV file. The expert can also subscribe for sensor data, that is, to periodically receive an email with a link to a CSV file containing the data that has been requested. Both links are valid for 24 h.

2.4.4. *Interface for the developer*

Typically, ExpoLIS developers access each sensor node using a custom graphical user interface developed in Python (the right-most representation in Fig. 12 depicts a screenshot of the tool). This interface allows the developer to monitor all sensor data in real-time, to download all stored logs, to configure the nodes operation, and even to reboot the supporting computing unit. The interface also shows the sensor node's IP address (published by the sensor node as a MQTT message in the state topic), which is useful whenever the user needs to connect to the sensor node via SSH.

Fig. 12. ExpoLIS graphical user interfaces, labelled according to the targeted user persona. The images are illustrative and these are not at scale.

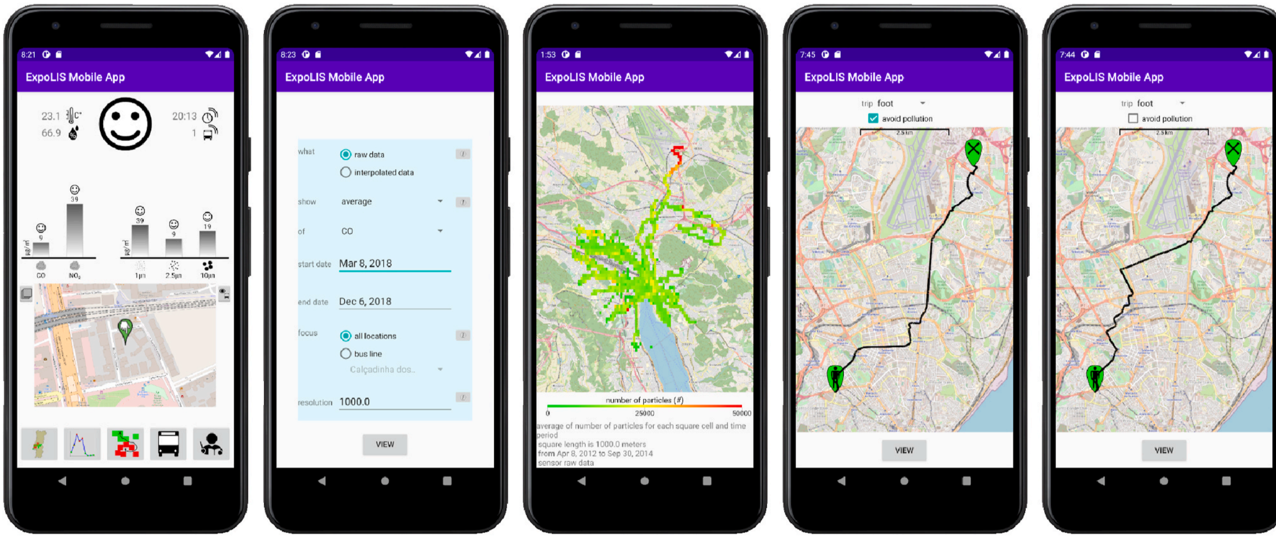

Fig. 13. Screenshots of the mobile application developed for the information-seeker, i.e., for pollution-aware people.

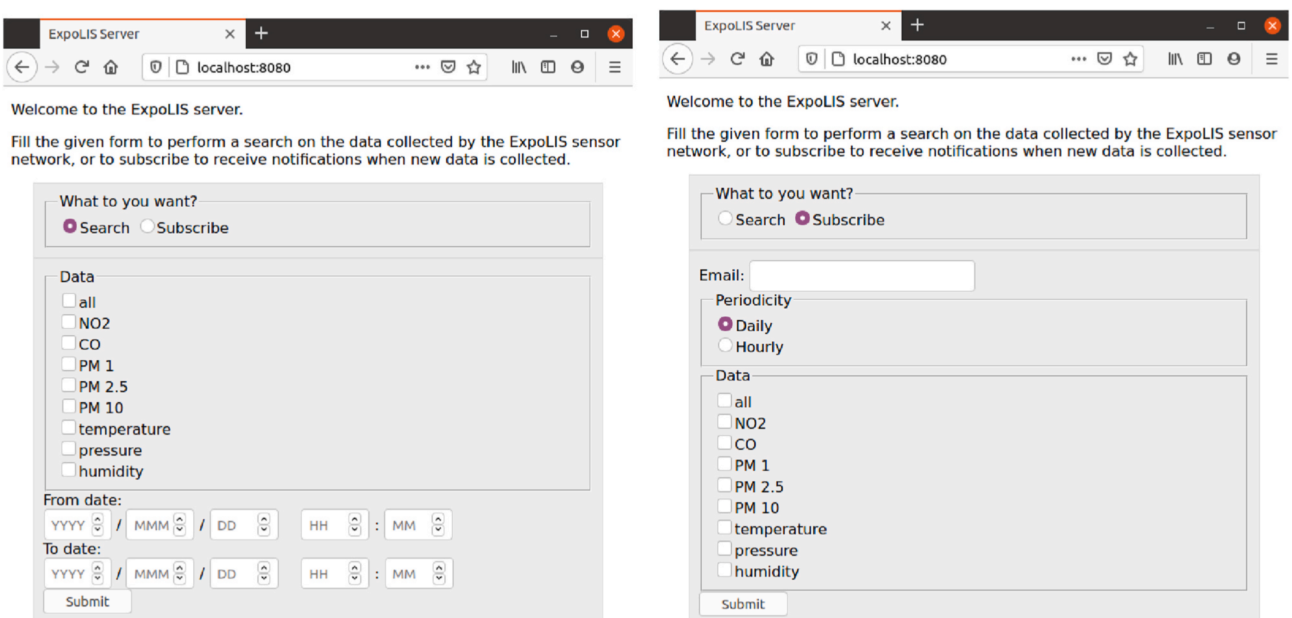

Fig. 14. The search (left image) and subscribe (right image) forms of the web component included in the ExpoLIS server.

3. Field experiments

To validate the design of the ExpoLIS sensor nodes, intercomparison experiments between our Prototype V_1 and a light scattering laser photometer DustTrak 8533 (TSI Inc., USA) were performed under static and dynamic conditions. The following details the experiments and the obtained results.

3.1. Static results

For the static condition, the intercomparison was peformed considering 1 min averages ($N = 310$) during the month of February 2020. Prototype V_1 showed a good correlation with the DustTrak monitor. The correlation coefficients (R^2) varied between 0.85, for PM10, and 0.96, for PM2.5. However, according to the Wilcoxon test, the concentrations given by Prototype V_1 were significantly lower than the ones measured by the DustTrak ($p < 0.05$), which means that the concentrations measured by Prototype V_1 must be corrected using the equations depicted in Fig. 15. Similarly, in a study developed in Warsaw by

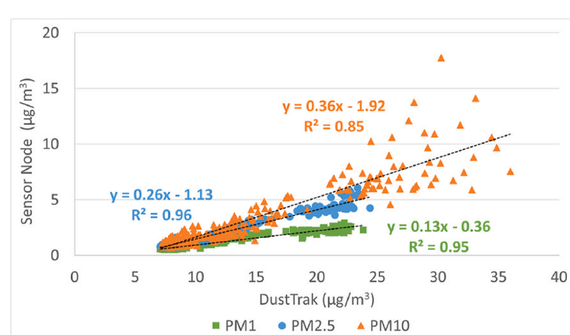

Fig. 15. Scatter plot of the linear regression of Prototype V_1, our sensor node equipped with an OPC-N3 from Alphasense, against the DustTrak 8533 for the mass concentrations of PM1, PM2.5, and PM10, under static conditions.

Kaliszewski et al. (2020), the particle number concentrations measured by the OPC-N3 were evaluated in comparison with an optical particle counter (AeroTrak 8220, TSI Inc., USA), and it was also verified that, although both concentrations showed a similar pattern, the OPC-N3 underestimated concentrations.

Another study developed in laboratory conditions with OPC-N2 (the model prior to the one used in our study) revealed measurable effects of particle size, particle type, and, principally, particle concentration on the sensor responses (Salimifard et al., 2020). The study also revealed a linear relationship between a low-cost sensor and a reference sensor. Furthermore, based on a field evaluation of several OPC-N2 with two different OPC used as reference, a portable aerosol spectrometer (PAS-1.108, GRIMM, USA), and an optical particle counter (TSI 3330, TSI Inc., USA), Crilley et al. (2018) showed that the equipment used for comparison influences the evaluation of the sensors' performance. This points out to the need for future work to evaluate the prototype's performance considering different levels of particulate concentrations and also using a reference method, that is, a gravimetric method.

3.2. Dynamic results

Although the performance of low-cost sensors is known to be very sensitive to their operating conditions, such as ambient temperature and humidity, they have the potential for quantifying urban air quality (Mead et al., 2013). To confirm the ability of Prototype V_1 to sample the airflow under dynamic situations, as predicted by the CFD analysis (see Section 2.2.3), Prototype V_1 was mounted on the roof of a car with its air intake tube attached to the DustTrak's air intake tube (see Fig. 16). The experiment consisted in performing a 100 km car trip in the Lisbon region (Portuguese capital city), in the late afternoon, without rain. The trip started in a rural city with light intensity traffic (Cartaxo), crossed Lisbon with intense traffic jams, and ended at a secondary urban city with medium intensity traffic (Setúbal).

A map of the PM10 mass concentrations observed during the car trip is depicted in Fig. 17. This map has been generated by the visualisation tool described in Section 2.4.1 and its colour coding post-processed (saturated) for the sake of readability. The map shows a higher concentration of particles in the portions of the trip with more intense traffic, as expected. These are promising results in the sense that they show that the system is sensitive to the presence of air pollution.

While the car was moving, PM1, PM2.5, and PM10 concentrations were measured by Prototype V_1 and DustTrak; the results are presented in Fig. 18. Although motion and other factors such as temperature and humidity may disturb particulate concentrations, the performance of Prototype V_1 showed to be satisfactory. Nevertheless, the correlations between Prototype V_1 and DustTrak were lower than the ones observed under static conditions (the R^2 varied between 0.57, for PM2.5, and 0.65, for PM1). As in the static experiments, the concentrations measured by Prototype V_1 were significantly lower than those measured by DustTrak ($p < 0.05$), indicating that a correction is also needed in this case. Although less accurate than the commercial alternative DustTrak, the proposed system is considerably lower in cost and has considerably more weather protection, making it more suitable for the task at hand.

4. Conclusions

The ExpoLIS System was presented as a contribution to the problem of affordable air quality monitoring in urban environments. The system being affordable, may easily be massively deployed for large-scale air quality monitoring. Affordability comes from using off-the-shelf consumable components, open-source software, open-hardware components, low-cost air quality sensing devices, and from exploiting the existing transportation infrastructure as a mobility platform for city-wise coverage. The expectation is that the resulting system manages to gather sensory data that can be used by citizens in their daily decision making processes, allowing them to opt for an healthier life style. For example, ExpoLIS includes a service that allows citizens to determine which routes result in less exposure to air pollution. Citizens are only akin to use air quality information if aware of its importance to their health. In this line, ExpoLIS also includes a game-like data visualisation service, aiming at raising awareness via engagement. ExpoLIS also includes data access interfaces for the environmental expert, so that bulk sensory data can be easily downloaded for later analysis and training of air pollution prediction models. Moreover, the availability of up-to-date information on urban air pollution can potentially help policy makers to identify and adopt cost-effective air pollution abatement measures.

At fixed air monitoring stations, sensing devices operate in considerably milder conditions than those that need to be handled by ExpoLIS sensor nodes. The signals acquired by sensors mounted on a vehicle's roof not only depend on the air pollutant levels, but also on a combination of effects, such as other interfering compounds, temperature, humidity, pressure, instability of the signal, and impact of the

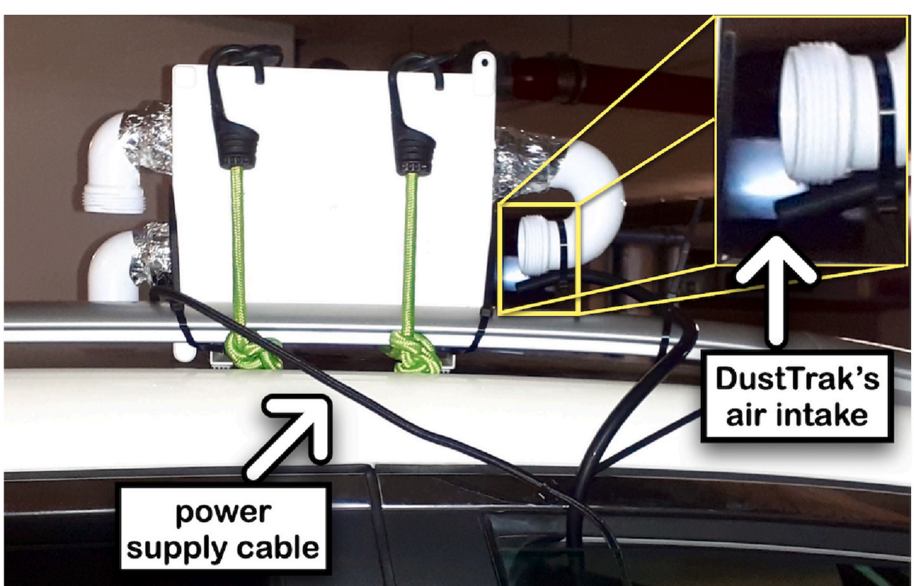

Fig. 16. Prototype V_1 attached to a car's roof, ready for the execution of real-life experiments under dynamic conditions.

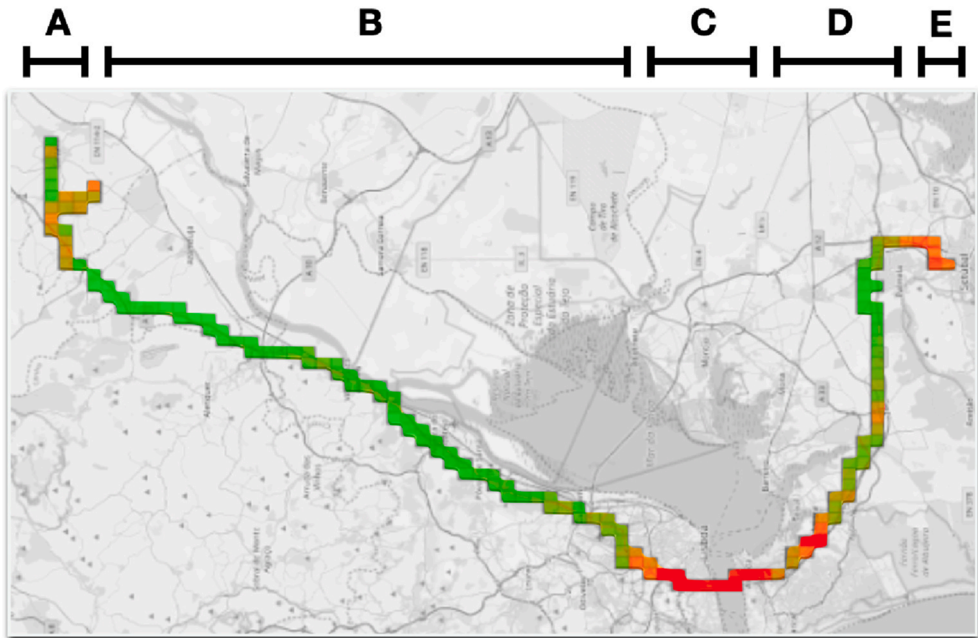

Fig. 17. Map of the PM10 mass concentrations observed by Prototype V_1 during a 100 km car trip in Lisbon region (capital city of Portugal). The car trip covered very disparate contexts and traffic intensities, represented by labels A, B, C, D, and E. A: Cartaxo, rural city with light intensity traffic. B: main highway with medium intensity traffic. C: Lisboa, main urban city with intense traffic jams. D: secondary high way with light intensity traffic. E: Setúbal, secondary urban city with medium intensity traffic.

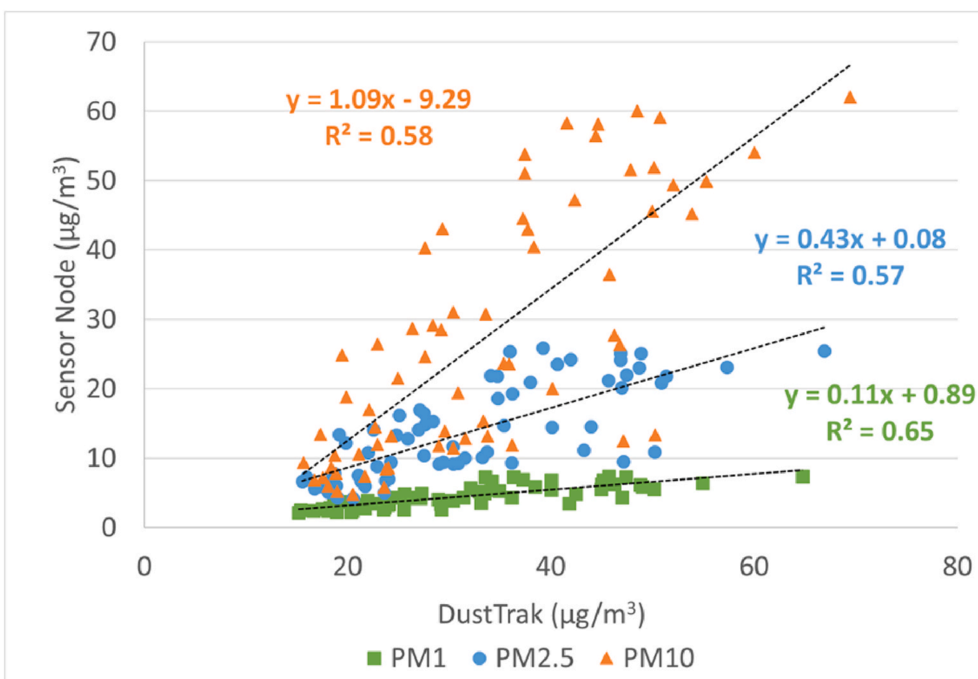

Fig. 18. Scatter plot of the linear regression of Prototype V_1, our sensor node equipped with an OPC-N3 from Alphasense, against the DustTrak 8533 for the mass concentrations of PM1, PM2.5, and PM10, under dynamic conditions.

movement. At high concentrations, as it is expected in city roads, the signal from the air pollutant is strong. However, at lower concentration levels, the signal can be weaker in comparison to the interfering effects, rendering simple corrections or calibrations not enough to guarantee quality results. Hence, to ensure that the sensors used in the ExpoLIS system continuously meet the data quality requirements, it is essential to subject them to rigorous and frequent quality control and calibration procedures. Field experiments have shown that the several components of the ExpoLIS system perform adequately. Under static conditions, the tested ExpoLIS sensor node showed a good correlation with the reference sensing device. The correlation coefficients varied between 0.85, for PM10, and 0.96, for PM2.5. Under dynamic conditions, the performance of the tested ExpoLIS sensor node was satisfactory. However, the correlations with the reference sensing device were lower when compared to those under static conditions. The correlation coefficient varied between 0.57, for PM2.5, and 0.65, for PM1.

Future work will be conducted along five main directions. Additional large-scale field experiences will be conducted to thoroughly compare the system's accuracy and robustness to existing high-cost alternative solutions (that are hardly replicable at scale) and static reference monitoring stations (that are limited to provide spatially sparse measurements). To perform this assessment, we will equip a fleet of city buses (as well as private vehicles) with our system alongside additional reference equipment for comparison purposes. The component for mechanical attachment of the sensor nodes to vehicles will be developed. It should be plug-and-play, avoid damaging the vehicle, and filter out potentially destructive vibrations. To better deal with dynamic conditions, we are considering the development of an air chamber, with controlled air intake and exhaust, capable of retaining air while being analysed by sensors. This should provide an extra degree of control over the airflow while the vehicle is moving. The system's server will also be extended to include web-services capable of providing third-party applications with access to data stored on the ExpoLIS server. Finally, the ExpoLIS system will be deployed in the city of Lisbon.

The ExpoLIS system cannot replace reference instruments, but the results obtained so far suggest that it can be used to complement conventional air quality monitoring, providing a new set of capabilities in the assessment of human exposure to air pollution.

CRediT authorship contribution statement

Pedro Santana: Supervision, Funding acquisition, Hardware, Software, Conceptualization, Investigation, Resources, Writing – original draft, Writing – review & editing. **Alexandre Almeida:** Funding acquisition, Hardware, Conceptualization, Investigation, Resources, Writing – original draft, Writing – review & editing. **Pedro Mariano:** Software, Conceptualization, Investigation, Resources, Writing – original draft, Writing – review & editing. **Carolina Correia:** Formal analysis, Conceptualization, Investigation, Resources, Writing – original draft, Writing – review & editing. **Vânia Martins:** Funding acquisition, Formal analysis, Conceptualization, Investigation, Resources, Writing – original draft, Writing – review & editing. **Susana Marta Almeida:** Supervision, Funding acquisition, Formal analysis, Conceptualization, Investigation, Resources, Writing – original draft, Writing – review & editing.

Declaration of competing interest

The authors declare that they have no known competing financial interests or personal relationships that could have appeared to influence the work reported in this paper.

Acknowledgements

We would like to thank our colleagues Tomás Brandão, José Moura, and Joaquim Reis for their helpful comments throughout the preparation and execution of the project. This study was supported by Portuguese Foundation for Science and Technology (FCT) through the project ExpoLIS (LISBOA-01-0145-FEDER-032088) and the contract CEECIND/04228/2018. Authors gratefully acknowledge the FCT support through the PhD grant UI/BD/150996/2021 and project UIDB/04349/2020.

References

EEA, 2019. Air Quality in Europe — 2019 Report, Tech. Rep. Publications Office of the European Union, Luxembourg.
Almeida, S.M., Silva, A., Sarmento, S., 2014. Effects of exposure to particles and ozone on hospital admissions for cardiorespiratory diseases in setúbal, Portugal. J. Toxicol. Environ. Health, Part A 77 (14–16), 837–848.
Banks, A., Briggs, E., Borgendale, K., Gupta, R., March 07, 2019. MQTT Version 5.0. OASIS Standard. https://docs.oasis-open.org/mqtt/mqtt/v5.0/mqtt-v5.0.html.
Carullo, A., Corbellini, S., Grassini, S., 2007. A remotely controlled calibrator for chemical pollutant measuring-units. IEEE Transactions on Instrumentation and Measurement 56 (4), 1212–1218.
Chatzidiakou, L., Krause, A., Popoola, O.A., Antonio, A.D., Kellaway, M., Han, Y., Squires, F.A., Wang, T., Zhang, H., Wang, Q., et al., 2019. Characterising low-cost sensors in highly portable platforms to quantify personal exposure in diverse environments. Atmospheric measurement techniques 12 (8), 4643–4657.
Correia, C., Martins, V., Cunha-Lopes, I., Faria, T., Diapouli, E., Eleftheriadis, K., Almeida, S., 2020. Particle exposure and inhaled dose while commuting in lisbon. Environ. Pollut. 257, 113547.
Crilley, L.R., Shaw, M., Pound, R., Kramer, L.J., Price, R., Young, S., Lewis, A.C., Pope, F. D., 2018. Evaluation of a low-cost optical particle counter (alphasense opc-n2) for ambient air monitoring. Atmospheric Measurement Techniques 11 (2), 709–720.
Devarakonda, S., Sevusu, P., Liu, H., Liu, R., Iftode, L., Nath, B., 2013. Real-time air quality monitoring through mobile sensing in metropolitan areas. In: Proceedings of the 2nd ACM SIGKDD International Workshop on Urban Computing, pp. 1–8.
Faria, T., Martins, V., Correia, C., Canha, N., Diapouli, E., Manousakas, M., Eleftheriadis, K., Almeida, S., 2020. Children's exposure and dose assessment to particulate matter in lisbon. Build. Environ. 171, 106666.
Gao, Y., Dong, W., Guo, K., Liu, X., Chen, Y., Liu, X., Bu, J., Chen, C., 2016. Mosaic: a low-cost mobile sensing system for urban air quality monitoring. In: Proceedings of the Annual IEEE International Conference on Computer Communications (INFOCOM). IEEE, pp. 1–9.
Hasenfratz, D., Saukh, O., Walser, C., Hueglin, C., Fierz, M., Arn, T., Beutel, J., Thiele, L., 2015. Deriving high-resolution urban air pollution maps using mobile sensor nodes. Pervasive Mob. Comput. 16, 268–285.
Kaliszewski, M., Włodarski, M., Młyńczak, J., Kopczyński, K., 2020. Comparison of low-cost particulate matter sensors for indoor air monitoring during covid-19 lockdown. Sensors 20 (24), 7290.
Linh, L.T.P., Kavalchuk, I., Kolbasov, A., Karpukhin, K., Terenchenko, A., 2020. The performance assessment of low-cost air pollution sensor in city and the prospect of the autonomous vehicle for air pollution reduction. IOP Conf. Ser. Mater. Sci. Eng. 819, 012018.
Luxen, D., Vetter, C., 2011. Real-time routing with openstreetmap data. In: Proceedings of the 19th ACM SIGSPATIAL International Conference on Advances in Geographic Information Systems, GIS '11. ACM, New York, NY, USA, pp. 513–516.
Mariano, P., Almeida, S.M., Santana, P., 2020. Pollution prediction model using data collected by a mobile sensor network. In: Proceedings of the 5th International Conference on Smart and Sustainable Technologies (SpliTech). IEEE, pp. 1–6.
Mead, M., Popoola, O., Stewart, G., Landshoff, P., Calleja, M., Hayes, M., Baldovi, J., McLeod, M., Hodgson, T., Dicks, J., et al., 2013. The use of electrochemical sensors for monitoring urban air quality in low-cost, high-density networks. Atmos. Environ. 70, 186–203.
Peng, R.D., Bell, M.L., 2010. Spatial misalignment in time series studies of air pollution and health data. Biostatistics 11 (4), 720–740.
Pope, C.A., Brook, R.D., Burnett, R.T., Dockery, D.W., 2011. How is cardiovascular disease mortality risk affected by duration and intensity of fine particulate matter exposure? an integration of the epidemiologic evidence. Air Quality, Atmosphere & Health 4 (1), 5–14.
Ripoll, A., Viana, M., Padrosa, M., Querol, X., Minutolo, A., Hou, K.M., Barcelo-Ordinas, J.M., García-Vidal, J., 2019. Testing the performance of sensors for ozone pollution monitoring in a citizen science approach. Sci. Total Environ. 651, 1166–1179.
Salimifard, P., Rim, D., Freihaut, J.D., 2020. Evaluation of low-cost optical particle counters for monitoring individual indoor aerosol sources. Aerosol. Sci. Technol. 54 (2), 217–231.
Santana, P., Almeida, A., Mariano, P., Correia, C., Martins, V., Almeida, S.M., 2020. An affordable vehicle-mounted sensing solution for mobile air quality monitoring. In: Proceedings of the 5th International Conference on Smart and Sustainable Technologies (SpliTech). IEEE, pp. 1–7.
Shindler, L., 2021. Development of a low-cost sensing platform for air quality monitoring: application in the city of rome. Environ. Technol. 42 (4), 618–631.
Teles, B., Mariano, P., Santana, P., 2020. Game-like 3d visualisation of air quality data. Multimodal Technologies and Interaction 4 (3), 54.
Weller, H.G., Tabor, G., Jasak, H., Fureby, C., 1998. A tensorial approach to computational continuum mechanics using object-oriented techniques. Comput. Phys. 12 (6), 620–631.
Yi, W.Y., Lo, K.M., Mak, T., Leung, K.S., Leung, Y., Meng, M.L., 2015. A survey of wireless sensor network based air pollution monitoring systems. Sensors 15 (12), 31392–31427.